

Light-Induced Paramagnetism in Colloidal Ag⁺-Doped CdSe Nanoplatelets

Arman Najafi,[¶] Manoj Sharma,[¶] Savas Delikanli, Arinjoy Bhattacharya, Joseph R. Murphy, James Pientka, Ashma Sharma, Alexander P. Quinn, Onur Erdem, Subash Kattel, Yusuf Kelestemur, Maksym V. Kovalenko, William D. Rice, Hilmi Volkan Demir,^{*} and Athos Petrou^{*}

Cite This: *J. Phys. Chem. Lett.* 2021, 12, 2892–2899

Read Online

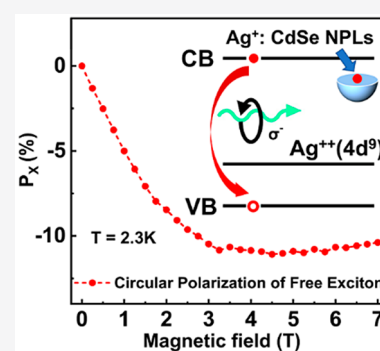
ACCESS |

Metrics & More

Article Recommendations

Supporting Information

ABSTRACT: We describe a study of the magneto-optical properties of Ag⁺-doped CdSe colloidal nanoplatelets (NPLs) that were grown using a novel doping technique. In this work, we used magnetic circularly polarized luminescence and magnetic circular dichroism spectroscopy to study light-induced magnetism for the first time in 2D solution-processed structures doped with nominally nonmagnetic Ag⁺ impurities. The excitonic circular polarization (P_x) and the exciton Zeeman splitting (ΔE_z) were recorded as a function of the magnetic field (B) and temperature (T). Both ΔE_z and P_x have a Brillouin-function-like dependence on B and T , verifying the presence of paramagnetism in Ag⁺-doped CdSe NPLs. The observed light-induced magnetism is attributed to the transformation of nonmagnetic Ag⁺ ions into Ag²⁺, which have a nonzero magnetic moment. This work points to the possibility of incorporating these nanoplatelets into spintronic devices, in which light can be used to control the spin injection.



Colloidal semiconductor nanocrystals (NCs) with a size-control capability at the monolayer level have been widely studied due to their interesting optical^{1–5} and electronic^{5–8} properties as well as their potential applications in light-emitting diodes,^{9–12} lasers,^{13–15} and light-harvesting devices.^{16–18} One can improve and control the optoelectronic properties of these NCs by incorporating impurities.¹⁹ In particular, magnetic properties are acquired by semiconductor NCs doped by Mn²⁺, a transition-metal ion with a half-filled d shell.^{20,21} Magnetically doped II–VI NCs, diluted magnetic semiconductor (DMS) systems, exhibit strong sp–d exchange interactions between the carrier and magnetic ion spins, resulting in enhanced conduction band (CB) and valence band (VB) Zeeman splittings in the presence of an external magnetic field.^{2,22–24} In addition, it has been shown that spontaneous magnetization can be induced in Mn²⁺-doped CdSe NCs in the absence of an external magnetic field.¹ The magneto-optical properties of magnetically doped NCs have been extensively investigated using a variety of techniques such as magnetic circularly polarized luminescence (MCPL),^{3,24,25} magnetic circular dichroism (MCD),^{22,26,27} time-resolved Faraday rotation,²⁸ resonant photoluminescence (PL),⁴ and time-resolved MCPL.²⁹

In II–VI semiconductors, Mn is an isovalent impurity and therefore cannot introduce excess carriers to the system, which is important for optoelectronic applications. In contrast, Cu and Ag dopants in II–VI semiconductor NCs act as acceptors that can capture photoexcited holes from the VB.^{30–33} The incorporation of Cu⁺ and Ag⁺ ions creates an acceptor state

above the top of the host VB. Transitions between the CB and the impurity state are responsible for the bright phosphor emission in these materials.^{30,34–44} Recent density functional theory calculations by Nelson et al.³⁹ indicate that in Cu⁺-doped CdSe NCs, the Cu⁺ impurity level has a predominantly 3d character with a substantial 4p contribution. In contrast, the Ag⁺ impurity in Ag⁺-doped CdSe NCs primarily consists of 4p orbitals in Se²⁻, with a small contribution from the Ag⁺ 4d orbitals.³⁹

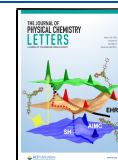
In addition to this important finding, it was discovered that Cu⁺-doped ZnSe/CdSe NCs and Ag⁺-doped CdSe NCs exhibit light-induced magnetism.^{37,40} The Cu⁺ and Ag⁺ ions—with a full d shell—capture a photogenerated hole from the VB and thus become Cu²⁺ and Ag²⁺ ions with one unpaired electron, resulting in a nonzero magnetic moment. MCD spectroscopy has been previously used to detect the magnetization in these NCs and to study its magnetic field and temperature dependence.^{37,40}

In this work, a new high-temperature synthesis method for doping 4 ML thick CdSe NPLs with Ag⁺ ions is described. This method has resulted in a dominant, efficient, and Stokes-shifted dopant-induced PL feature. Detailed elemental and

Received: February 3, 2021

Accepted: March 12, 2021

Published: March 16, 2021



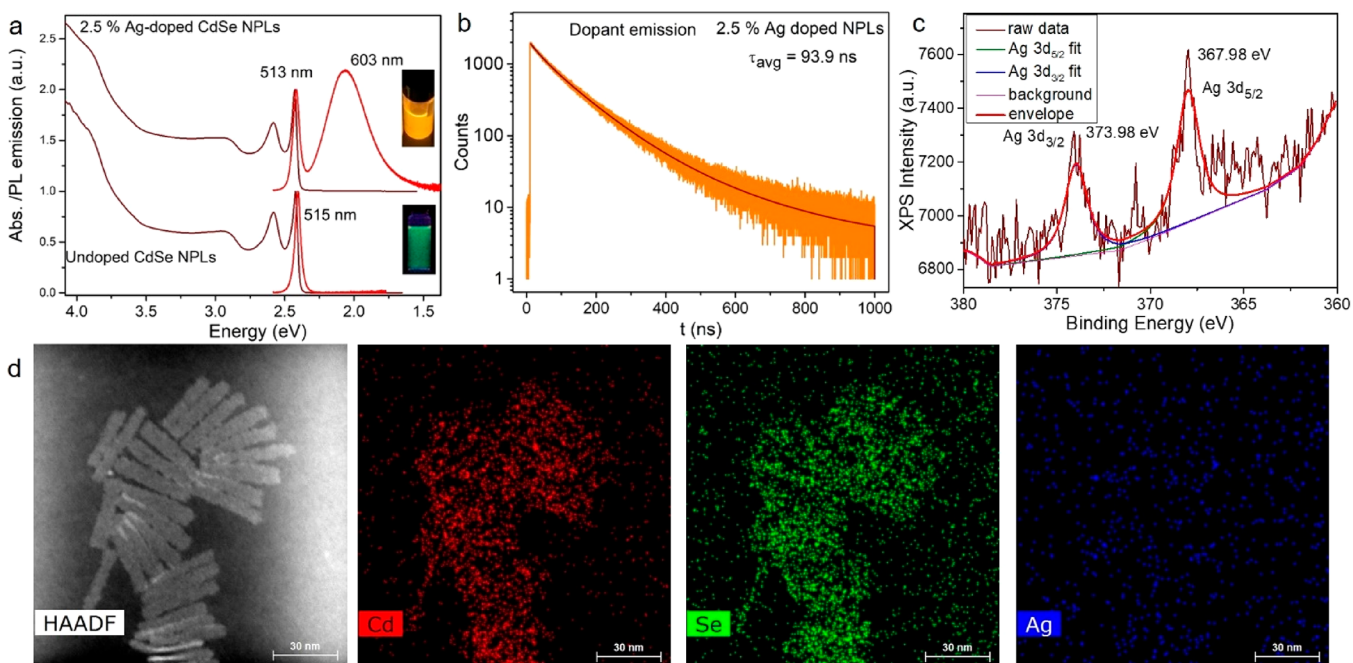


Figure 1. (a) Room-temperature UV–visible absorption and PL emission spectra of Ag⁺-doped (top) and undoped (bottom) 4 ML thick CdSe NPLs. Stokes-shifted emission at 603 nm from the doped sample is associated with the CB to Ag⁺ impurity level transition. (b) Decay profile of Ag-dopant-activated emission for doped NPLs. (c) High-resolution XPS spectra of Ag 3d states for Ag⁺-doped CdSe NPLs. (d) HAADF–TEM and EDS images of Ag⁺-doped CdSe NPLs for Cd, Se, and Ag.

optical characterizations confirmed the successful doping by Ag⁺ ions in 4 ML thick CdSe host NPLs. We have applied MCPL and MCD spectroscopies to study light-induced magnetism by investigating the temperature (T) and magnetic field (B) dependence of the free-exciton luminescence circular polarization, P_X , and the exciton Zeeman splitting, ΔE_Z , in Ag⁺-doped CdSe NPLs. The 2D character of NPLs and their high optical quality result in the presence of a sharp and strong PL feature associated with the ground-state exciton. In previously studied Ag⁺-doped NCs, one could not measure the MCPL due to the weakness of the band-edge excitonic emission.⁴⁰ Both P_X and ΔE_Z in our Ag⁺-doped CdSe NPLs follow a Brillouin-like dependence on the magnetic field and the temperature—evidence of the presence of light-induced paramagnetism. The energy E_- of the right circularly polarized (RCP, σ_-) free-exciton component is below the energy E_+ of the left circularly polarized (LCP, σ_+) component. As a result, the observed circular polarization P_X (Zeeman splitting is defined as $E_+ - E_-$) of the free exciton is negative (positive), that is, opposite in sign to the circular polarization and Zeeman splitting of Mn²⁺-doped NCs and NPLs.^{2,3,24,45} The results of our MCPL measurements are in agreement with those from our MCD experiments.

Room-Temperature PL and Absorption. In Figure 1a, we show the room-temperature absorption and emission spectra for the Ag-doped sample (top) and the undoped sample (bottom). The PL spectrum of the undoped sample contains only band-edge excitonic emission, which is typical for 4 ML CdSe NPLs. Emission from the doped sample shows an additional emission feature (at 603 nm) below the excitonic emission associated with the CB to Ag⁺ impurity level transition in Ag⁺-doped CdSe NCs^{39,40} and CdSe NPLs.^{41,46} The intensity of this Stokes-shifted emission feature can be tuned by changing the dopant precursor amount. The typical PL quantum efficiencies of Ag⁺-doped CdSe NPLs synthesized by our hot injection

nucleation doping method range from 50 to 80%. The time-resolved PL decay curves for Ag⁺-doped CdSe NPLs at the dopant-activated emission wavelengths were recorded. Figure 1b shows the decay curve for the Ag-doped sample at the dopant emission (at 603 nm). This emission shows a typical long lifetime with an average value of 93.9 ns that is fitted with three exponentials. The long lifetime for the Ag-dopant-induced emission for these Ag⁺-doped CdSe NPLs is similar to that in reported works for Ag-doped CdSe NCs;^{40,41} however, further analysis is needed to fully understand this efficient dopant-induced emission with different doping percentages. The excitonic emission for doped and undoped NPLs shows an average lifetime of 2.30 and 2.13 ns, respectively. The detailed fitting parameters of the PL components are given in the Supporting Information (Table S1, Figure S1).

To elementally characterize the presence of Ag⁺ dopant ions in the host CdSe NPLs, we have conducted X-ray photoelectron spectroscopy (XPS) and high-angle annular dark-field–scanning transmission electron microscopy (HAADF–STEM)-based energy-dispersive X-ray spectroscopy (EDS) measurements. The high-resolution XPS spectrum of a doped sample is shown in Figure 1c. It contains features associated with the 3d_{5/2} and 3d_{3/2} states of Ag 3d states, which is clear evidence of successful Ag⁺ doping in the CdSe host NPLs. The high-resolution XPS profiles for host elements Cd and Se are shown in Figure S2. Figure 1d contains an HAADF–TEM image of the Ag-doped sample. It exhibits rectangular morphology with a high aspect ratio (5.0–7.0 depending on the growth time). Moreover, EDS maps of Cd, Se, and Ag also show the presence of these metal ions in doped NPLs; however, because of the low resolution of EDS mapping for our doping ranges, it is difficult to see the clear contrast for Ag dopant ions through EDS mapping. To quantify Ag doping levels in the studied doped samples, inductively coupled plasma mass spectrometry (ICP–MS) measurements were

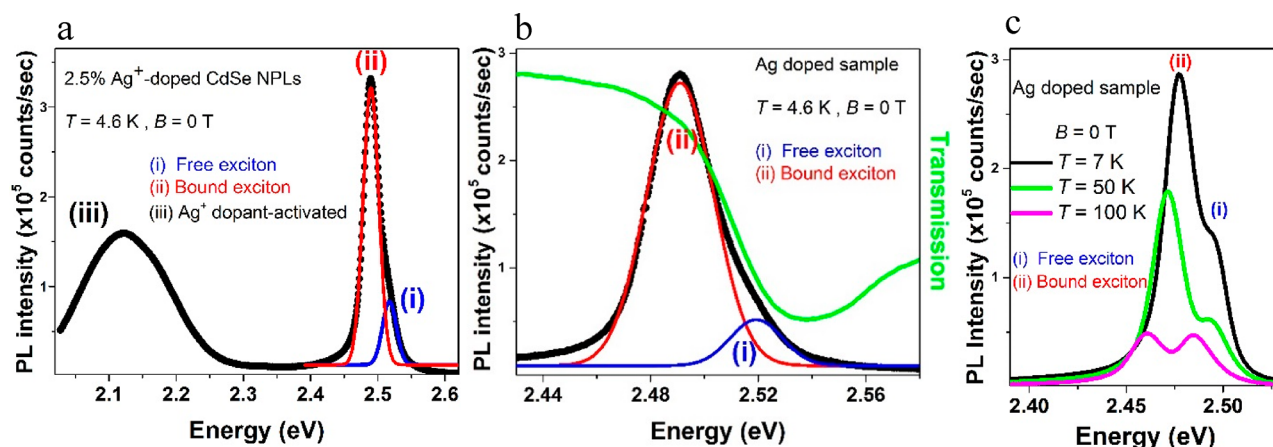


Figure 2. (a) Zero-field photoluminescence (PL) of Ag^+ -doped CdSe NPLs at $T = 4.6$ K. Features (i) and (ii) are attributed to band-edge excitonic emissions, and feature (iii) is Ag^+ -dopant-activated emission. (b) The same PL as that in panel a is shown in the vicinity of excitonic emissions. Feature (i) in blue and feature (ii) in red are recognized as free-exciton and bound-exciton emissions, respectively. The transmission spectrum is shown in green, which coincides with feature (i). (c) Temperature dependence of excitonic features (i) and (ii) at 7 (black), 50 (green), and 100 K (magenta) shows the increasing intensity of feature (i) relative to feature (ii).

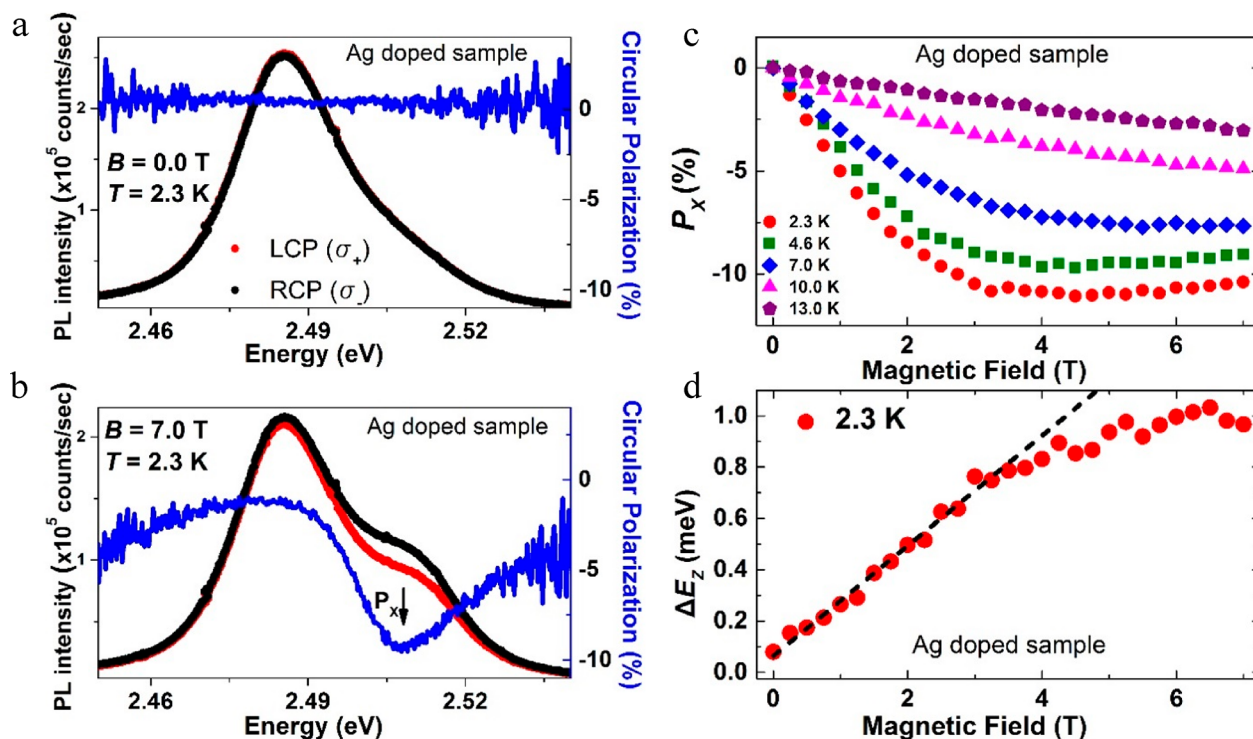


Figure 3. (a) Left circularly polarized (LCP) (red dots) and right circularly polarized (RCP) (black dots) components of PL from the Ag-doped sample at $T = 2.3$ K and $B = 0$ T. Circular polarization is shown with a blue line that is nearly zero in the vicinity of band-edge emission. (b) LCP and RCP components of PL and circular polarization (P_x) (blue line) from the Ag-doped sample at $T = 2.3$ K and $B = 7$ T. A distinct circular polarization feature at free-exciton energy (P_x) is indicated with a black vertical arrow. (c) P_x as a function of magnetic field (B) at several temperatures (T) for the Ag-doped sample. P_x shows a Brillouin function-like dependence on B and T . (d) Free-exciton Zeeman splitting (ΔE_z) (the difference in the energies of the LCP and RCP components of free-exciton PL) as a function of B at $T = 2.3$ K for the Ag-doped sample. ΔE_z up to +1 meV at $T = 2.3$ K is observed.

conducted. The atomic percentages of Ag dopant ions with respect to total cations were estimated to be 2.5% for excessively cleaned samples. Typically, all doped samples were cleaned with ethanol approximately five times before the measurements were conducted.

Low-Temperature PL and Magnetic Circularly Polarized Luminescence. The zero-field PL at $T = 4.6$ K from the Ag-doped sample shown in Figure 2a contains three features: two

band-edge luminescence (features (i) and (ii)) at 2.52 and 2.49 eV and the Ag^+ dopant-activated emission (feature (iii)) at 2.12 eV. In Figure 2b, the energy scale is expanded in the vicinity of the excitonic features for clarity, and it shows the band-edge luminescence fitted with two Gaussian line shapes: Feature (i) (blue) at 2.52 eV and feature (ii) (red) at 2.49 eV are identified as being due to the free exciton and bound exciton, respectively. The identification was made on the basis

of a comparison with the transmission spectrum, also shown in Figure 2b (green line). The broadening of the free and bound excitons could be attributed to a variety of reasons such as the finite temperature, interaction with residual impurities, and strain variation within the nanoplatelets. Whereas the PL component at 2.52 eV has a strong absorption signature, the PL component at 2.49 eV does not have a corresponding absorption feature. Furthermore, when the sample temperature is raised, the intensity of the 2.52 eV component relative to the intensity of the 2.49 eV component increases. This is shown in Figure 2c, in which we plot the PL spectra in the vicinity of features (i) and (ii) for three temperatures: 7 (black), 50 (green), and 100 K (magenta). A band-edge emission spectrum from the undoped sample is shown in Figure S3.

To investigate the magnetization of Ag⁺-doped CdSe NPLs, we used MCPL spectroscopy, and the results are summarized in Figure 3. The low-temperature ($T = 2.3$ K) LCP (σ_+) and RCP (σ_-) components of band-edge PL and its circular polarization (blue lines) as a function of photon energy for the Ag-doped sample at $B = 0$ and 7 T are shown in Figure 3a,b, respectively. The circular polarization is defined as $100 \times (I_+ - I_-)/(I_+ + I_-)$, where I_+ (I_-) is the intensity of the σ_+ (σ_-) PL component. The zero-field polarization of Figure 3a is featureless and has a value close to zero. In contrast, when a magnetic field is applied, the polarization acquires a negative value at the energy of the free exciton (feature (i) in Figure 2b), as indicated by a vertical arrow in Figure 3b. We also observe that the circular polarization at the energy of the bound exciton (feature (ii) in Figure 2b) is very small.

In Figure 3c, the free-exciton circular polarization, P_X , is plotted as a function of magnetic field, B , for several temperatures for the Ag-doped sample. P_X follows a Brillouin-like dependence on T and B . At $T = 2.3$ K, $|P_X|$ monotonically increases with B and saturates after 3 T at 10%. We note that doping CdSe NPLs with Ag flips the sign of P_X compared with Mn²⁺-doped NPLs.^{24,29,45} In contrast with the Brillouin-like behavior of the Ag-doped sample, the P_X of the undoped sample exhibits a linear dependence on B , as is shown in Figure S4.

In Figure 3d, we plot the free-exciton Zeeman splitting (ΔE_Z) as a function of B at $T = 2.3$ K for the Ag-doped sample. ΔE_Z is defined as $\Delta E_Z = E_+ - E_-$ where E_+ (E_-) is the energy of the σ_+ (σ_-) PL free-exciton component extracted from the Gaussian fitting of feature (i) shown in Figure 2b. ΔE_Z increases monotonically with B and saturates after 3 T at ~ 1 meV. The positive Zeeman splitting ($\Delta E_Z > 0$), that is, $E_+ > E_-$, is in agreement with the circular polarization negative sign ($P_X < 0$).

The results shown in Figure 3 provide evidence of the presence of light-induced magnetism in the Ag⁺-doped CdSe NPLs. Both P_X and ΔE_Z follow a Brillouin-like dependence on B and T . In particular, P_X and ΔE_Z saturate at low temperature for $B > 3$ T. This is not the case for the undoped CdSe NPLs.

We interpret the appearance of paramagnetism in our Ag-doped sample following the model of ref 40, also shown in Figure 4. Under illumination, electrons are photoexcited into the CB (step (i)). A fraction of these electrons get trapped on surface defect states (step (ii)). As a result, we have a majority of photogenerated holes in the VB. A number of these holes are captured by the nonmagnetic Ag⁺ 4d¹⁰ state, which is transformed into the magnetic 4d⁹ Ag²⁺ state (step (iii)). Electron and hole spins are aligned by the sp–d exchange interaction with the Ag²⁺ spins. Recombination of CB electrons

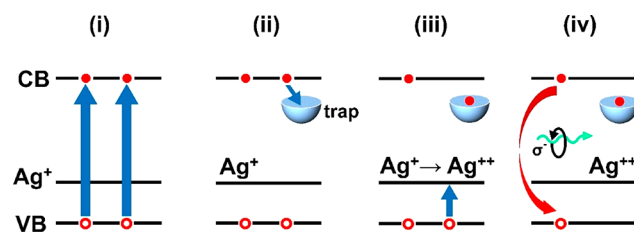


Figure 4. Schematic of the light-induced magnetism process in Ag⁺-doped CdSe NPLs. Step (i): Electrons and holes are photoexcited. Step (ii): A fraction of photogenerated electrons are trapped in surface defect states. Step (iii): A number of photogenerated holes are captured by Ag⁺, which is transformed into paramagnetic Ag²⁺. Step (iv): Electrons and holes whose spins are partially aligned by the sp–d interaction with spins of Ag²⁺ recombine and create circularly polarized PL.

with VB holes results in the emission of excitonic PL, circularly polarized as σ_- (step (iv)).

The free exciton is a simple electron–hole hydrogenic system. The bound exciton, on the contrary, is a more complex system that is localized on an impurity atom. We speculate that the residual interactions of exciton electron and hole spins with the spins of the impurity mask the subtle effects of the sp–d interaction with the Ag²⁺ spins and result in the nearly zero circular polarization of the bound exciton.

The results shown in Figure 3 were collected after a 45 min illumination period during which P_X was monitored. We found that P_X initially changes with illumination and after ~ 30 min reaches a steady-state value. In Figure 3, we present the steady-state values for P_X . This time delay has been previously observed in Ag⁺:CdSe NCs, and it has been attributed by Pinchetti et al.⁴⁰ to the presence of surface defect states positioned in energy above the Fermi level that trap the photoexcited CB electrons, leaving the Ag impurities in their magnetic Ag²⁺ state. The work of Pinchetti et al.⁴⁰ utilized two light beams; a weak probe beam for the MCD measurement and a stronger UV beam that drives the Ag⁺ \rightarrow Ag²⁺ process. In our experiment, we use a single above-gap laser beam that drives Ag²⁺ formation and also excites the PL.

We note that in previously studied II–VI NCs and NPLs doped with Mn, $\Delta E_Z < 0$ and $P_X > 0$,^{2,3,24,29,45} which are opposite in sign to those in our Ag⁺-doped CdSe NPLs. This sign reversal has been previously observed in Cu⁺-doped ZnSe–CdSe NCs and attributed to the nature of the interaction between holes in the VB (p-type) and unpaired electrons in the d shell.³⁷ Unlike the s–d interaction, in which only a $1/r$ potential exchange interaction is involved, there is a contribution due to hybridization of the d shell with the p holes that competes with the potential p–d exchange interaction. This competition could result in the sign reversal of Zeeman splittings and related circular polarization.^{22,37,47}

Magnetic Circular Dichroism. To help confirm the light-induced magnetization of Ag dopants previously described, we performed MCD spectroscopy at low temperatures and high magnetic fields. In brief, MCD measures the normalized difference in RCP and LCP absorption, which, with the aid of a magnetic field applied in the Faraday geometry, can measure the effective Zeeman splitting between field-split spin states, ΔE_Z . If the light-induced, metastable Ag²⁺ state is created through the mechanism described first by Pinchetti et al.⁴⁰ and shown in Figure 4, then we expect sp–d spin exchange to occur between the CBs/VBs of the CdSe NPL and the

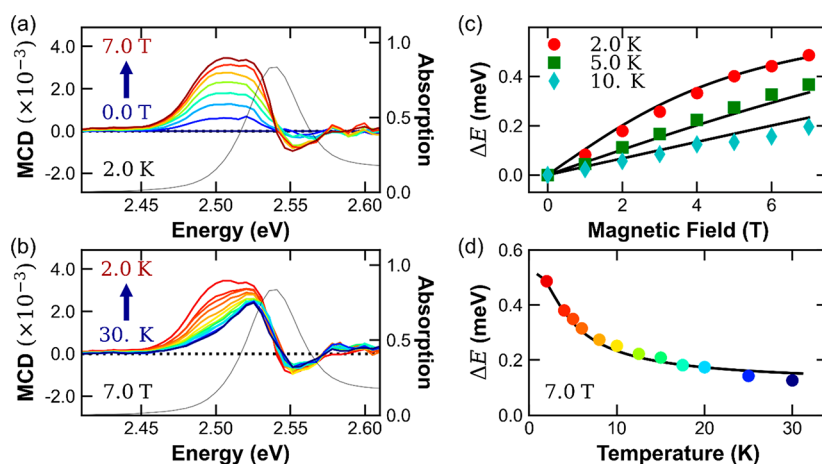


Figure 5. (a) Absorption spectrum (right y axis) and field-dependent MCD spectra for Ag⁺-doped CdSe NPLs at 2.0 K. The spectra, which are collected in 1 T increments, show a saturation-like behavior at high fields, which strongly suggests the exciton is nondiamagnetic. (b) 2.0 K absorption spectrum (right y axis) and temperature-dependent MCD spectra for Ag⁺-doped CdSe NPLs. The clear increase in the MCD with decreasing temperature shows that the Zeeman splitting is paramagnetic. ΔE_Z as a function of (c) field for 2.0, 5.0, and 10 K and (d) temperature at 7 T. The black lines are simultaneously fitted to these four data sets using eq 1, confirming the DMS behavior of Ag⁺-doped CdSe NPLs.

unpaired d electrons of the Ag dopant. Because this behavior relies on the dopant magnetization, the effective Zeeman splitting of the exciton not only depends on T but also saturates above a given B . Therefore, the bare exciton Zeeman splitting, $g_{\text{ex}}\mu_B B$, is modified by the sp–d exchange through a Brillouin-like dependence on the ratio of the magnetic dopant energy to the thermal energy⁴⁷

$$\Delta E_Z = g_{\text{ex}}\mu_B B + \Delta E_{\text{spd}} B_f \left(\frac{g_{\text{Ag}}\mu_B JB}{k_B T} \right) \quad (1)$$

where ΔE_{spd} is the magnitude of sp–d exchange splitting, $B_f(x)$ is the Brillouin function modeling the projection of the Ag spins along B for a given x , and $J = 1/2$ for Ag²⁺.

In Figure 5a, we plot the MCD spectra associated with the free exciton of Ag⁺-doped CdSe NPLs around 2.54 eV at 2.0 K as a function of B in steps of 1 T. As with Ag⁺:CdSe and Mn-doped CdSe colloidal NCs,^{1–3,40} the lowest MCD feature sharply increases in magnitude, saturates at high fields and low temperatures, and has a distinctly non-derivative-like shape around the excitonic absorption features, which is shown in gray for $B = 0$ T. These behaviors in themselves do not directly indicate DMS behavior in Ag⁺-doped CdSe NPLs, but they do strongly suggest its presence in our system.

Figure 5b, which shows MCD as a function of temperature at 7.0 T, provides a more direct test of DMS physics because the Ag ion magnetization changes with temperature. Unlike a diamagnetic exciton that exhibits no dependence on temperature,^{20,28} we observe a clear increase in the MCD around the 1s absorption feature as temperature decreases. Converting the MCD spectra into ΔE_Z values, we plot the effective Zeeman splitting as a function of the magnetic field and temperature in Figure 5c,d. As expected from the spectra previously described, we see that at 2.0 K saturates as the field is increased (Figure 5c), which sharply diverges from the traditional diamagnetic Zeeman behavior. Similarly, Figure 5d shows that the temperature-dependent at 7.0 T nonlinearly drops with increasing T . We note that a small discrepancy exists between the values obtained from MCPL (Figure 3d) and MCD (Figure 5c,d). Although the estimated effective Zeeman splitting for both determinations of Ag⁺-doped CdSe NPLs is

on the order of hundreds of microelectronvolts, errors from fitting congested spectra for both experiments contribute to small errors in determining.

To better understand the observed DMS behavior, we simultaneously fit the four data sets shown in Figure 5c,d using eq 1. As the excellent agreement of the black fitting curves to the data indicates, we are able to describe all of the MCD data with the same parameters ($g_{\text{Ag}} = 1.3$, $\Delta E_{\text{spd}} = 0.40$ meV, $g_{\text{ex}} = 0.27$). Interestingly, our value of g_{Ag} exactly matches that obtained by Pinchetti et al.⁴⁰ and is in line with that of Ag-doped bulk ZnSe.⁴⁸ The relatively small value of ΔE_{spd} (e.g., a factor of 5 smaller than that in ref 40) is likely an indication of low Ag ion concentration, poor CdSe–exciton–Ag-dopant wave function overlap, or both. These findings confirm the MCPL results previously discussed and unambiguously show that DMS physics can be used to describe the light-induced spin magnetization of Ag⁺-doped CdSe NPLs at low temperatures.

In conclusion, we have described a new method for doping colloidal CdSe NPLs with Ag. In this work, we used both MCPL and MCD spectroscopies to study the light-induced magnetism and optical manipulation of magnetism in Ag⁺-doped CdSe NPLs. The observation of a strong and sharp PL feature associated with the ground-state free exciton allowed us to focus on the excitonic recombination channel. We measured the exciton Zeeman splitting, ΔE_Z , and the resulting circular polarization, P_X , as a function of the magnetic field, B , and temperature, T . ΔE_Z and $|P_X|$ dependence on B and T is consistent with Brillouin paramagnetism in our NPLs. There is a monotonic increase in both parameters with B followed by saturation for $B > 3.0$ T. ΔE_Z and $|P_X|$ decrease with increasing temperature. This work demonstrates that MCPL is a useful tool for the study of light-induced magnetism in our Ag⁺-doped CdSe NPLs and related 2D systems. These 2D NPLs doped with nominally nonmagnetic impurities exhibiting light-induced magnetization properties present a novel platform for 2D solution-processed spin-based semiconductor devices and spintronic applications in which the properties of the device components can be modulated by light.

■ ASSOCIATED CONTENT**SI Supporting Information**

The Supporting Information is available free of charge at <https://pubs.acs.org/doi/10.1021/acs.jpcllett.1c00398>.

Experimental methods, room-temperature decay profile and fitting parameters of undoped and Ag⁺-doped CdSe NPLs, high-resolution XPS spectra of Ag⁺-doped CdSe NPLs, and PL and magnetic-field dependence of the excitonic circular polarization of undoped CdSe NPLs at low temperature (PDF)

■ AUTHOR INFORMATION**Corresponding Authors**

Hilmi Volkan Demir – Luminous! Centre of Excellence for Semiconductor Lighting and Displays, School of Electrical and Electronic Engineering and Division of Physics and Applied Physics, School of Physical and Mathematical Sciences, Nanyang Technological University, Singapore 639798; Department of Electrical and Electronics Engineering and Department of Physics, UNAM-Institute of Materials Science and Nanotechnology, Bilkent University, 06800 Ankara, Turkey; orcid.org/0000-0003-1793-112X; Email: hvdemir@ntu.edu.sg

Athos Petrou – Department of Physics, University at Buffalo SUNY, Buffalo, New York 14260, United States; Email: petrou@buffalo.edu

Authors

Arman Najafi – Department of Physics, University at Buffalo SUNY, Buffalo, New York 14260, United States; orcid.org/0000-0002-8022-5095

Manoj Sharma – Luminous! Centre of Excellence for Semiconductor Lighting and Displays, School of Electrical and Electronic Engineering and Division of Physics and Applied Physics, School of Physical and Mathematical Sciences, Nanyang Technological University, Singapore 639798; Department of Electrical and Electronics Engineering and Department of Physics, UNAM-Institute of Materials Science and Nanotechnology, Bilkent University, 06800 Ankara, Turkey; orcid.org/0000-0001-5215-9740

Savas Delikanli – Luminous! Centre of Excellence for Semiconductor Lighting and Displays, School of Electrical and Electronic Engineering and Division of Physics and Applied Physics, School of Physical and Mathematical Sciences, Nanyang Technological University, Singapore 639798; Department of Electrical and Electronics Engineering and Department of Physics, UNAM-Institute of Materials Science and Nanotechnology, Bilkent University, 06800 Ankara, Turkey; orcid.org/0000-0002-0613-8014

Arinjoy Bhattacharya – Department of Physics, University at Buffalo SUNY, Buffalo, New York 14260, United States; orcid.org/0000-0002-8019-4233

Joseph R. Murphy – Department of Chemistry and Physics, Southeast Missouri State University, Cape Girardeau, Missouri 63701, United States; Department of Physics and Astronomy, University of Wyoming, Laramie, Wyoming 82071, United States; orcid.org/0000-0002-9947-995X

James Pientka – Department of Physics, St. Bonaventure University, St. Bonaventure, New York 14778, United States; orcid.org/0000-0003-3167-4246

Ashma Sharma – Luminous! Centre of Excellence for Semiconductor Lighting and Displays, School of Electrical

and Electronic Engineering and Division of Physics and Applied Physics, School of Physical and Mathematical Sciences, Nanyang Technological University, Singapore 639798

Alexander P. Quinn – Department of Physics, University at Buffalo SUNY, Buffalo, New York 14260, United States

Onur Erdem – Department of Electrical and Electronics Engineering and Department of Physics, UNAM-Institute of Materials Science and Nanotechnology, Bilkent University, 06800 Ankara, Turkey

Subash Kattel – Department of Physics and Astronomy, University of Wyoming, Laramie, Wyoming 82071, United States

Yusuf Kelestemur – Department of Chemistry and Applied Biosciences, ETH Zürich, CH-8093 Zürich, Switzerland; Department of Metallurgical and Materials Engineering, Atilim University, Ankara 06830, Turkey; orcid.org/0000-0003-1616-2728

Maksym V. Kovalenko – Department of Chemistry and Applied Biosciences, ETH Zürich, CH-8093 Zürich, Switzerland; Empa–Swiss Federal Laboratories for Materials Science and Technology, CH-8600 Dübendorf, Switzerland; orcid.org/0000-0002-6396-8938

William D. Rice – Department of Physics and Astronomy, University of Wyoming, Laramie, Wyoming 82071, United States; orcid.org/0000-0003-4548-4187

Complete contact information is available at: <https://pubs.acs.org/doi/10.1021/acs.jpcllett.1c00398>

Author Contributions

[†]A.N. and M.S. contributed equally to this work.

Notes

The authors declare no competing financial interest.

■ ACKNOWLEDGMENTS

A.P. acknowledges support from the NSF MRI Award 1726303. M.S. and H.V.D. acknowledge the financial support from the Singapore National Research Foundation under the Programs of NRF-NRFI2016-08, NRF-CRP14-2014-03, and the Science and Engineering Research Council, Agency for Science, Technology, and Research (A*STAR) of Singapore. H.V.D. acknowledges additional financial support from the TUBA. M.V.K. and Y.K. acknowledge financial support from the European Union's Horizon 2020 research and innovation program under the Marie Skłodowska-Curie grant no. 798697. We acknowledge the support of the Scientific Center for Optical and Electron Microscopy (ScopeM) of the Swiss Federal Institute of Technology ETHZ.

■ REFERENCES

- (1) Beaulac, R.; Schneider, L.; Archer, P. I.; Bacher, G.; Gamelin, D. R. Light-Induced Spontaneous Magnetization in Doped Colloidal Quantum Dots. *Science* **2009**, *325*, 973–976.
- (2) Beaulac, R.; Archer, P. I.; Gamelin, D. R. Luminescence in Colloidal Mn²⁺-Doped Semiconductor Nanocrystals. *J. Solid State Chem.* **2008**, *181*, 1582–1589.
- (3) Viswanatha, R.; Pietryga, J. M.; Klimov, V. I.; Crooker, S. A. Spin-Polarized Mn²⁺ Emission from Mn-Doped Colloidal Nanocrystals. *Phys. Rev. Lett.* **2011**, *107*, 067402.
- (4) Rice, W. D.; Liu, W.; Pinchetti, V.; Yakovlev, D. R.; Klimov, V. I.; Crooker, S. A. Direct Measurements of Magnetic Polarons in Cd_{1-x}Mn_xSe Nanocrystals from Resonant Photoluminescence. *Nano Lett.* **2017**, *17*, 3068–3075.

- (5) Smith, A. M.; Mohs, A. M.; Nie, S. Tuning the Optical and Electronic Properties of Colloidal Nanocrystals by Lattice Strain. *Nat. Nanotechnol.* **2009**, *4*, 56–63.
- (6) Sargent, E. H. Solar Cells, Photodetectors, and Optical Sources from Infrared Colloidal Quantum Dots. *Adv. Mater.* **2008**, *20*, 3958–3964.
- (7) Shirasaki, Y.; Supran, G. J.; Bawendi, M. G.; Bulović, V. Emergence of Colloidal Quantum-Dot Light-Emitting Technologies. *Nat. Photonics* **2013**, *7*, 13–23.
- (8) Kagan, C. R.; Lifshitz, E.; Sargent, E. H.; Talapin, D. V. Building Devices from Colloidal Quantum Dots. *Science* **2016**, *353* (6302), aac5523.
- (9) Yang, P.; Ando, M.; Taguchi, T.; Murase, N. Highly Luminescent CdSe/Cd_xZn_{1-x}S Quantum Dots with Narrow Spectrum and Widely Tunable Wavelength. *J. Phys. Chem. C* **2011**, *115*, 14455–14460.
- (10) Pal, B. N.; Ghosh, Y.; Brovelli, S.; Laocharoensuk, R.; Klimov, V. I.; Hollingsworth, J. A.; Htoon, H. ‘Giant’ CdSe/CdS Core/Shell Nanocrystal Quantum Dots As Efficient Electroluminescent Materials: Strong Influence of Shell Thickness on Light-Emitting Diode Performance. *Nano Lett.* **2012**, *12*, 331–336.
- (11) Chen, Z.; Nadal, B.; Mahler, B.; Aubin, H.; Dubertret, B. Quasi-2D Colloidal Semiconductor Nanoplatelets for Narrow Electroluminescence. *Adv. Funct. Mater.* **2014**, *24*, 295–302.
- (12) Fan, F.; Kanjanaboos, P.; Saravanapavanantham, M.; Beauregard, E.; Ingram, G.; Yassitepe, E.; Adachi, M. M.; Voznyy, O.; Johnston, A. K.; Walters, G.; Kim, G.-H.; Lu, Z.-H.; Sargent, E. H. Colloidal CdSe_{1-x}S_x Nanoplatelets with Narrow and Continuously-Tunable Electroluminescence. *Nano Lett.* **2015**, *15*, 4611–4615.
- (13) She, C.; Fedin, I.; Dolzhenkov, D. S.; Demortière, A.; Schaller, R. D.; Pelton, M.; Talapin, D. V. Low-Threshold Stimulated Emission Using Colloidal Quantum Wells. *Nano Lett.* **2014**, *14*, 2772–2777.
- (14) Guzelurk, B.; Kelestemur, Y.; Olutas, M.; Delikanli, S.; Demir, H. V. Amplified Spontaneous Emission and Lasing in Colloidal Nanoplatelets. *ACS Nano* **2014**, *8*, 6599–6605.
- (15) Liao, C.; Xu, R.; Xu, Y.; Zhang, C.; Xiao, M.; Zhang, L.; Lu, C.; Cui, Y.; Zhang, J. Ultralow-Threshold Single-Mode Lasing from Phase-Pure CdSe/CdS Core/Shell Quantum Dots. *J. Phys. Chem. Lett.* **2016**, *7*, 4968–4976.
- (16) Bang, J.; Park, J.; Lee, J. H.; Won, N.; Nam, J.; Lim, J.; Chang, B. Y.; Lee, H. J.; Chon, B.; Shin, J.; Park, J. B.; Choi, J. H.; Cho, K.; Park, S. M.; Joo, T.; Kim, S. ZnTe/ZnSe (Core/Shell) Type-II Quantum Dots: Their Optical and Photovoltaic Properties. *Chem. Mater.* **2010**, *22*, 233–240.
- (17) Kelestemur, Y.; Olutas, M.; Delikanli, S.; Guzelurk, B.; Akgul, M. Z.; Demir, H. V. Type-II Colloidal Quantum Wells: CdSe/CdTe Core/Crown Heteronanoplatelets. *J. Phys. Chem. C* **2015**, *119*, 2177–2185.
- (18) Kelestemur, Y.; Guzelurk, B.; Erdem, O.; Olutas, M.; Erdem, T.; Usanmaz, C. F.; Gungor, K.; Demir, H. V. CdSe/CdSe_{1-x}Te_x Core/Crown Heteronanoplatelets: Tuning the Excitonic Properties without Changing the Thickness. *J. Phys. Chem. C* **2017**, *121*, 4650–4658.
- (19) Erwin, S. C.; Zu, L.; Haftel, M. I.; Efros, A. L.; Kennedy, T. A.; Norris, D. J. Doping Semiconductor Nanocrystals. *Nature* **2005**, *436*, 91–94.
- (20) Norris, D. J.; Yao, N.; Charnock, F. T.; Kennedy, T. A. High-Quality Manganese-Doped ZnSe Nanocrystals. *Nano Lett.* **2001**, *1*, 3–7.
- (21) Beaulac, R.; Archer, P. I.; Ochsenbein, S. T.; Gamelin, D. R. Mn²⁺-Doped CdSe Quantum Dots: New Inorganic Materials for Spin-Electronics and Spin-Photonics. *Adv. Funct. Mater.* **2008**, *18*, 3873–3891.
- (22) Bussian, D. A.; Crooker, S. A.; Yin, M.; Brynda, M.; Efros, A. L.; Klimov, V. I. Tunable Magnetic Exchange Interactions in Manganese-Doped Inverted Core-Shell ZnSe-CdSe Nanocrystals. *Nat. Mater.* **2009**, *8*, 35–40.
- (23) Vlaskin, V. A.; Beaulac, R.; Gamelin, D. R. Dopant-Carrier Magnetic Exchange Coupling in Colloidal Inverted Core/Shell Semiconductor Nanocrystals. *Nano Lett.* **2009**, *9*, 4376–4382.
- (24) Delikanli, S.; Akgul, M. Z.; Murphy, J. R.; Barman, B.; Tsai, Y.; Scrace, T.; Zhang, P.; Bozok, B.; Hernández-Martínez, P. L.; Christodoulides, J.; Cartwright, A. N.; Petrou, A.; Demir, H. V. Mn²⁺-Doped CdSe/CdS Core/Multishell Colloidal Quantum Wells Enabling Tunable Carrier-Dopant Exchange Interactions. *ACS Nano* **2015**, *9*, 12473–12479.
- (25) Shornikova, E. V.; Biadala, L.; Yakovlev, D. R.; Feng, D. H.; Sapega, V. F.; Flipo, N.; Golovatenko, A. A.; Semina, M. A.; Rodina, A. V.; Mitioglu, A. A.; Ballottin, M. V.; Christianen, P. C. M.; Kusrayev, Y. G.; Nasilowski, M.; Dubertret, B.; Bayer, M. Electron and Hole G-Factors and Spin Dynamics of Negatively Charged Excitons in CdSe/CdS Colloidal Nanoplatelets with Thick Shells. *Nano Lett.* **2018**, *18*, 373–380.
- (26) Barrows, C. J.; Fainblat, R.; Gamelin, D. R. Excitonic Zeeman Splittings in Colloidal CdSe Quantum Dots Doped with Single Magnetic Impurities. *J. Mater. Chem. C* **2017**, *5*, 5232–5238.
- (27) Muckel, F.; Delikanli, S.; Hernández-Martínez, P. L.; Priesner, T.; Lorenz, S.; Ackermann, J.; Sharma, M.; Demir, H. V.; Bacher, G. Sp-d Exchange Interactions in Wave Function Engineered Colloidal CdSe/Mn:CdS Hetero-Nanoplatelets. *Nano Lett.* **2018**, *18*, 2047–2053.
- (28) Rice, W. D.; Liu, W.; Baker, T. A.; Sinitsyn, N. A.; Klimov, V. I.; Crooker, S. A. Revealing Giant Internal Magnetic Fields Due to Spin Fluctuations in Magnetically Doped Colloidal Nanocrystals. *Nat. Nanotechnol.* **2016**, *11*, 137–142.
- (29) Najafi, A.; Tarasek, S.; Delikanli, S.; Zhang, P.; Norden, T.; Shendre, S.; Sharma, M.; Bhattacharya, A.; Taghipour, N.; Pientka, J.; Demir, H. V.; Petrou, A.; Thomay, T. CdSe/CdMnS Nanoplatelets with Bilayer Core and Magnetically Doped Shell Exhibit Switchable Excitonic Circular Polarization: Implications for Lasers and Light-Emitting Diodes. *ACS Appl. Nano Mater.* **2020**, *3*, 3151–3156.
- (30) Sahu, A.; Kang, M. S.; Kompch, A.; Notthoff, C.; Wills, A. W.; Deng, D.; Winterer, M.; Frisbie, C. D.; Norris, D. J. Electronic Impurity Doping in CdSe Nanocrystals. *Nano Lett.* **2012**, *12*, 2587–2594.
- (31) Sharma, M.; Gungor, K.; Yeltik, A.; Olutas, M.; Guzelurk, B.; Kelestemur, Y.; Erdem, T.; Delikanli, S.; McBride, J. R.; Demir, H. V. Near-Unity Emitting Copper-Doped Colloidal Semiconductor Quantum Wells for Luminescent Solar Concentrators. *Adv. Mater.* **2017**, *29*, 1700821.
- (32) Sharma, M.; Olutas, M.; Yeltik, A.; Kelestemur, Y.; Sharma, A.; Delikanli, S.; Guzelurk, B.; Gungor, K.; McBride, J. R.; Demir, H. V. Understanding the Journey of Dopant Copper Ions in Atomically Flat Colloidal Nanocrystals of CdSe Nanoplatelets Using Partial Cation Exchange Reactions. *Chem. Mater.* **2018**, *30*, 3265–3275.
- (33) Sharma, A.; Sharma, M.; Gungor, K.; Olutas, M.; Dede, D.; Demir, H. V. Near-Infrared-Emitting Five-Monolayer Thick Copper-Doped CdSe Nanoplatelets. *Adv. Opt. Mater.* **2019**, *7*, 1900831.
- (34) Bhaumik, S.; Ghosh, B.; Pal, A. J. Color Tunable Light-Emitting Diodes Based on Copper Doped Semiconducting Nanocrystals. *Appl. Phys. Lett.* **2011**, *99*, 083106.
- (35) Srivastava, B. B.; Jana, S.; Pradhan, N. Doping Cu in Semiconductor Nanocrystals: Some Old and Some New Physical Insights. *J. Am. Chem. Soc.* **2011**, *133*, 1007–1015.
- (36) Viswanatha, R.; Brovelli, S.; Pandey, A.; Crooker, S. A.; Klimov, V. I. Copper-Doped Inverted Core/Shell Nanocrystals with “Permanent” Optically Active Holes. *Nano Lett.* **2011**, *11*, 4753–4758.
- (37) Pandey, A.; Brovelli, S.; Viswanatha, R.; Li, L.; Pietryga, J. M.; Klimov, V. I.; Crooker, S. A. Long-Lived Photoinduced Magnetization in Copper-Doped ZnSe-CdSe Core-Shell Nanocrystals. *Nat. Nanotechnol.* **2012**, *7*, 792–797.
- (38) Knowles, K. E.; Nelson, H. D.; Kilburn, T. B.; Gamelin, D. R. Singlet-Triplet Splittings in the Luminescent Excited States of Colloidal Cu⁺:CdSe, Cu⁺:InP, and CuInS₂ Nanocrystals: Charge-

Transfer Configurations and Self-Trapped Excitons. *J. Am. Chem. Soc.* **2015**, *137*, 13138–13147.

(39) Nelson, H. D.; Hinterding, S. O. M.; Fainblat, R.; Creutz, S. E.; Li, X.; Gamelin, D. R. Mid-Gap States and Normal vs Inverted Bonding in Luminescent Cu⁺- and Ag⁺-Doped CdSe Nanocrystals. *J. Am. Chem. Soc.* **2017**, *139*, 6411–6421.

(40) Pinchetti, V.; Di, Q.; Lorenzon, M.; Camellini, A.; Fasoli, M.; Zavelani-Rossi, M.; Meinardi, F.; Zhang, J.; Crooker, S. A.; Brovelli, S. Excitonic Pathway to Photoinduced Magnetism in Colloidal Nanocrystals with Nonmagnetic Dopants. *Nat. Nanotechnol.* **2018**, *13*, 145–151.

(41) Dufour, M.; Izquierdo, E.; Livache, C.; Martinez, B.; Silly, M. G.; Pons, T.; Lhuillier, E.; Delerue, C.; Ithurria, S. Doping as a Strategy to Tune Color of 2D Colloidal Nanoplatelets. *ACS Appl. Mater. Interfaces* **2019**, *11*, 10128–10134.

(42) Liu, B.; Sharma, M.; Yu, J.; Shendre, S.; Hettiarachchi, C.; Sharma, A.; Yeltik, A.; Wang, L.; Sun, H.; Dang, C.; Demir, H. V. Light-Emitting Diodes with Cu-Doped Colloidal Quantum Wells: From Ultrapure Green, Tunable Dual-Emission to White Light. *Small* **2019**, *15*, 1901983.

(43) Yu, J.; Sharma, M.; Delikanli, S.; Birowosuto, M. D.; Demir, H. V.; Dang, C. Mutual Energy Transfer in a Binary Colloidal Quantum Well Complex. *J. Phys. Chem. Lett.* **2019**, *10*, 5193–5199.

(44) Sharma, M.; Delikanli, S.; Demir, H. V. Two-Dimensional CdSe-Based Nanoplatelets: Their Heterostructures, Doping, Photo-physical Properties, and Applications. *Proc. IEEE* **2020**, *108* (5), 655–675.

(45) Shornikova, E. V.; Yakovlev, D. R.; Tolmachev, D. O.; Ivanov, V. Yu.; Kalitukha, I. V.; Sapega, V. F.; Kudlacik, D.; Kusrayev, Y. G.; Golovatenko, A. A.; Shendre, S.; Delikanli, S.; Demir, H. V.; Bayer, M. Magneto-Optics of Excitons Interacting with Magnetic Ions in CdSe/CdMnS Colloidal Nanoplatelets. *ACS Nano* **2020**, *14*, 9032–9041.

(46) Khan, A. H.; Pinchetti, V.; Tanghe, I.; Dang, Z.; Martín-García, B.; Hens, Z.; Van Thourhout, D.; Geiregat, P.; Brovelli, S.; Moreels, I. Tunable and Efficient Red to Near-Infrared Photoluminescence by Synergistic Exploitation of Core and Surface Silver Doping of CdSe Nanoplatelets. *Chem. Mater.* **2019**, *31*, 1450–1459.

(47) Furdyna, J. K. Diluted Magnetic Semiconductors. *J. Appl. Phys.* **1988**, *64*, R29–R64.

(48) Poolton, N. R. J.; Davies, J. J.; Nicholls, J. E.; Fitzpatrick, B. J. An ODMR Investigation of Silver Doped ZnSe. *J. Cryst. Growth* **1985**, *72*, 336–341.